



Synthesis, characterization, cytotoxicity, apoptotic inducing activity, cellular uptake, interaction of DNA binding and antioxidant activity studies of ruthenium(II) complexes

Yun-Jun Liu^{a,*}, Zhen-Hua Liang^a, Xian-Lan Hong^b, Zheng-Zheng Li^a, Jun-Hua Yao^c, Hong-Liang Huang^{d,*}

^aSchool of Pharmacy, Guangdong Pharmaceutical University, Guangzhou 510006, PR China

^bDepartment of Chemistry, Shaoguan University, Shaoguan 512005, PR China

^cInstrumentation Analysis and Research Center, Sun Yat-Sen University, Guangzhou 510275, PR China

^dSchool of Life Science and Biopharmaceutical, Guangdong Pharmaceutical University, Guangzhou 510006, PR China

ARTICLE INFO

Article history:

Received 28 January 2011

Received in revised form 7 October 2011

Accepted 4 January 2012

Available online 13 January 2012

Keywords:

Ruthenium(II) complexes

DNA-binding

Cytotoxicity

Apoptosis

Cellular uptake

Antioxidant activity

ABSTRACT

Two new ligands APIP, HAPIP and their relative ruthenium(II) complexes [Ru(bpy)₂(APIP)](ClO₄)₂ **1** and [Ru(bpy)₂(HAPIP)](ClO₄)₂ **2** have been synthesized and characterized. The DNA binding constants for complexes **1** and **2** have been determined to be 6.08 (±0.29) × 10⁴ M⁻¹ and 1.78 (±0.30) × 10⁵ M⁻¹. The results suggest that these complexes intercalate between the base pairs of DNA. The cytotoxicity of complexes has been evaluated by MTT assay. The apoptosis assay was carried out with AO/EB staining methods. The cellular uptake was observed under fluorescence microscopy. The studies on the mechanism of photocleavage demonstrate that superoxide anion radical (O₂^{•-}) and singlet oxygen (¹O₂) may play an important role. The antioxidant activity against hydroxyl radical (•OH) was also studied.

© 2012 Elsevier B.V. All rights reserved.

1. Introduction

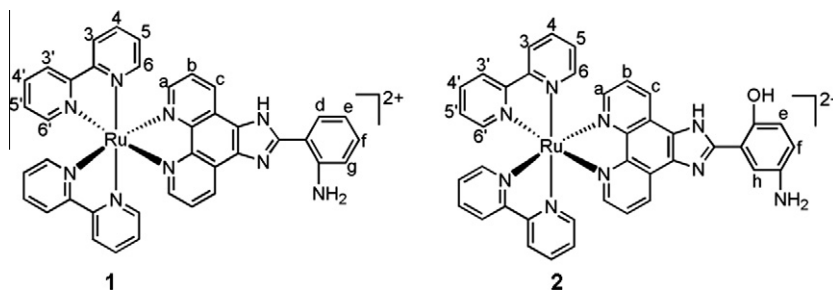
In recent years, many researchers have focused on the studies of interaction of small molecules with DNA [1–7]. DNA is generally the primary intracellular target of anticancer drugs, so the interaction between small molecules and DNA can cause DNA damage in cancer cells, blocking the division of cancer cells, and resulting in cell death [8,9]. The studies on the interaction of transition metal complexes with DNA continue to attract the attention of researcher due to their importance in design and development of synthetic restriction enzymes, chemotherapeutic drugs and DNA foot printing agents, DNA cleavage agents and DNA “molecular light switch” [10–14]. Generally, small molecule can interact with DNA through the three non-covalent modes: groove binding, intercalation, and

external static electronic effects. The studies on the DNA-binding behaviors of ruthenium complexes have attracted great attention, and some of them exhibit interesting properties. However, little is known about their in vitro behaviors. Only a few studies have focused on their intracellular accumulation and antiproliferative properties [15–19]. These studies found some complexes to possess excellent antitumor activity and might be as potential candidate for drugs. In fact, the activity of many anticancer, antimalarial and antibacterial agents finds its origin in intercalative interactions with DNA [20]. In this study, we report the synthesis, characterization, DNA-binding, cytotoxicity, apoptosis, cellular uptake and antioxidant activity of two new ruthenium(II) polypyridyl complexes [Ru(bpy)₂(APIP)](ClO₄)₂ **1** (bpy = 2,2'-bipyridine, APIP = 2-(2-aminophenyl)imidazo[4,5-f][1,10]phenanthroline) and [Ru(bpy)₂(HAPIP)](ClO₄)₂ **2** (HAPIP = 2-(2-hydroxyl-5-aminophenyl)imidazo[4,5-f][1,10]phenanthroline, Scheme 1). The DNA-binding behaviors were studied by spectroscopic titration, viscosity measurements, thermal denaturation and photocleavage. The spectroscopic titration and viscosity changes of calf thymus DNA (CT DNA) show these complexes interact with DNA through intercalative mode. The cytotoxicity of complexes has been evaluated by MTT (3-(4,5-dimethylthiazol-2-yl)-2,5-diphenyltetrazolium bromide) assay. The apoptosis of BEL-7402 cells induced by Ru(II) complexes was investigated. The retardation assay of pGL 3 plasmid DNA by

Abbreviations: APIP, 2-(2-aminophenyl)imidazo[4,5-f][1,10]phenanthroline; HAPIP, 2-(2-hydroxyl-5-aminophenyl)imidazo[4,5-f][1,10]phenanthroline; CT DNA, calf thymus DNA; bpy, 2,2'-bipyridine; AO, acridine orange; EB, ethidium bromide; DMSO, dimethylsulfoxide; RPMI, Roswell Park Memorial Institute; MLCT, metal to ligand charge transfer; Tris, tris(hydroxymethyl)aminomethane; ES-MS, electrospray mass spectroscopy; MTT, 3-(4,5-dimethylthiazol-2-yl)-2,5-diphenyltetrazolium bromide.

* Corresponding authors.

E-mail addresses: lyjche@163.com (Y.-J. Liu), hhongliang@163.com (H.-L. Huang).



Scheme 1. The structure of complexes.

complexes **1** and **2** was also explored. The cellular uptake shows that complexes can easily enter into the cytoplasm and accumulate in the nuclei. The antioxidant activity of ligands and complexes was performed by hydroxyl radical scavenging method. The studies on the mechanism of photocleavage reveal that singlet oxygen ($^1\text{O}_2$) and superoxide anion radical ($\text{O}_2^{\cdot-}$) may play an important role.

2. Experimental

2.1. Materials and methods

Calf thymus DNA (CT DNA) was obtained from the Sino-American Biotechnology Company. pBR 322 DNA was obtained from Shanghai Sangon Biological Engineering & Services Co., Ltd. Dimethyl sulfoxide (DMSO) and RPMI 1640 were purchased from Sigma. Cell lines of BEL-7402 (hepatocellular), HepG-2 (hepatocellular) and MCF-7 (breast cancer) were purchased from American Type Culture Collection, agarose and ethidium bromide were obtained from Aldrich. $\text{RuCl}_3 \cdot x\text{H}_2\text{O}$ was purchased from Kunming Institution of Precious Metals. 1,10-Phenanthroline was obtained from Guangzhou Chemical Reagent Factory. Doubly distilled water was used to prepare buffers (5 mM tris(hydroxymethylaminomethane)-HCl, 50 mM NaCl, pH 7.2). A solution of calf thymus DNA in the buffer gave a ratio of UV absorbance at 260 and 280 nm of ca. 1.8–1.9:1, indicating that the DNA was sufficiently free of protein [21]. The DNA concentration per nucleotide was determined by absorption spectroscopy using the molar absorption coefficient ($6600 \text{ M}^{-1} \text{ cm}^{-1}$) at 260 nm [22].

Microanalysis (C, H, and N) was carried out with a Perkin-Elmer 240Q elemental analyzer. Fast atom bombardment (FAB) mass spectra were recorded on a VG ZAB-HS spectrometer in a 3-nitrobenzyl alcohol matrix. Electropray mass spectra (ES-MS) were recorded on a LCQ system (Finnigan MAT, USA) using methanol as mobile phase. The spray voltage, tube lens offset, capillary voltage and capillary temperature were set at 4.50 kV, 30.00 V, 23.00 V and 200 °C, respectively, and the quoted m/z values are for the major peaks in the isotope distribution. ^1H NMR spectra were recorded on a Varian-500 spectrometer. All chemical shifts were given relative to tetramethylsilane (TMS). UV–Vis spectra were recorded on a Shimadzu UV-3101PC spectrophotometer at room temperature. Luminescence spectra were recorded on a Shimadzu RF-2000 spectrophotometer at room temperature.

2.2. Synthesis of ligands and complexes

2.2.1. 2-(2-Aminophenyl)imidazo[4,5-f][1,10]phenanthroline (APIP)

A mixture of 2-(2-nitrophenyl)imidazo[4,5-f][1,10]phenanthroline (0.171 g, 0.5 mmol) (NPIP) [23] was completely dissolved in ethanol (50 cm^3) with stirring for 1 h. Then the Pd/C (0.20 g, 10% Pd) and $\text{NH}_2\text{NH}_2 \cdot \text{H}_2\text{O}$ (8 cm^3) were added in the above solution and refluxed for 6 h. The hot solution was filtered and evaporated to remove the solvent under reduced pressure. The red compound

obtained was washed with cold ethanol and dried at 50 °C in vacuo. Yield: 73%. *Anal. Calc.* for $\text{C}_{19}\text{H}_{13}\text{N}_5$: C, 73.30; H, 4.21; N, 22.49. Found: C, 73.16; H, 4.13; N, 22.38%. FAB–MS: $m/z = 312 [\text{M}+1]^+$. ^1H NMR (500 MHz, $\text{DMSO}-d_6$): 9.05 (d, 2H, H_c , $J = 8.0$ Hz), 8.98 (d, 2H, H_a , $J = 8.2$ Hz), 8.02–8.05 (m, 2H, H_b), 7.83 (d, 1H, H_g , $J = 8.0$ Hz), 7.18–7.35 (m, 1H, H_e), 6.92 (d, 1H, H_f , $J = 8.0$ Hz), 6.74 (t, 1H, H_d , $J = 7.6$ Hz), 3.36 (s, 2H, H_{NH_2}).

2.2.2. 2-(2-Hydroxyl-5-aminophenyl)imidazo[4,5-f][1,10]phenanthroline (HAPIP)

This compound was prepared with the similar method described for APIP, with 2-(2-hydroxyl-5-nitrophenyl)imidazo[4,5-f][1,10]phenanthroline (0.179 g, 0.5 mmol) [24] in place of APIP. Yield: 72%. *Anal. Calc.* for $\text{C}_{19}\text{H}_{13}\text{N}_5\text{O}$: C, 69.72; H, 4.00; N, 21.39. Found: C, 69.60; H, 4.13; N, 21.52%. FAB–MS: $m/z = 328 [\text{M}+1]^+$. ^1H NMR (500 MHz, $\text{DMSO}-d_6$): 9.06 (d, 2H, H_c , $J = 8.2$ Hz), 8.98 (d, 2H, H_a , $J = 7.5$ Hz), 7.87 (dd, 2H, H_b , $J = 8.0$ Hz), 7.43 (d, 1H, H_d , $J = 8.0$ Hz), 6.84 (d, 1H, H_f , $J = 8.6$ Hz), 6.73–6.75 (m, 1H, H_e), 4.78 (s, 1H, H_{OH}), 3.39 (s, 2H, H_{NH_2}).

2.2.3. Synthesis of $[\text{Ru}(\text{bpy})_2(\text{APIP})](\text{ClO}_4)_2$ (**1**)

$[\text{Ru}(\text{bpy})_2(\text{NPIP})](\text{ClO}_4)_2$ (0.485 g, 0.5 mmol) [23] was completely dissolved in acetonitrile. Then the ethanol of 45 cm^3 , Pd/C (0.20 g, 10% Pd) and $\text{NH}_2\text{NH}_2 \cdot \text{H}_2\text{O}$ (8 cm^3) were added in the above solution and refluxed under argon for 8 h to give a clear red solution. Upon cooling, a red precipitate was obtained by dropwise addition of saturated aqueous NaClO_4 solution. The crude product was purified by column chromatography on a neutral alumina with a mixture of CH_3CN -toluene (3:1, v/v) as eluant. The mainly red band was collected. The solvent was removed under reduced pressure and a red powder was obtained. Yield: 71%. *Anal. Calc.* for $\text{C}_{39}\text{H}_{29}\text{N}_9\text{Cl}_2\text{O}_8\text{Ru}$: C, 50.71; H, 3.16; N, 13.65. Found: C, 50.48; H, 3.28; N, 13.59%. ESI-MS [CH_3CN , m/z]: 723.4 ($[\text{M}-2\text{ClO}_4-\text{H}]^+$), 362.3 ($[\text{M}-2\text{ClO}_4]^{2+}$). ^1H NMR (500 MHz, $\text{DMSO}-d_6$): δ 8.91 (dd, 4H, $\text{H}_{3,3'}$, $J = 8.4$, $J = 8.5$ Hz), 8.80 (d, 2H, H_c , $J = 8.2$ Hz), 8.21–8.27 (m, 4H, $\text{H}_{4,4'}$), 8.14 (t, 2H, $J = 7.5$ Hz), 7.85 (d, 4H, $\text{H}_{6,6'}$, $J = 6.0$ Hz), 7.58–7.66 (m, 2H, H_b), 7.36 (t, 4H, $\text{H}_{5,5'}$, $J = 7.6$ Hz), 7.20 (t, 1H, H_d , $J = 7.5$ Hz), 6.98–7.03 (m, 1H, H_f), 6.92 (t, 1H, H_e , $J = 7.8$ Hz), 6.72 (t, 1H, H_g , $J = 7.8$ Hz), 3.37 (s, 2H, H_{NH_2}).

2.2.4. Synthesis of $[\text{Ru}(\text{bpy})_2(\text{HAPIP})](\text{ClO}_4)_2$ (**2**)

A mixture of *cis*- $[\text{Ru}(\text{bpy})_2\text{Cl}_2] \cdot 2\text{H}_2\text{O}$ [25] (0.260 g, 0.5 mmol) and HAPIP (0.164 g, 0.5 mmol) in ethanol (30 cm^3) was refluxed under argon for 8 h to give a clear red solution. Upon cooling, a red precipitate was obtained by dropwise addition of saturated aqueous NaClO_4 solution. The crude product was purified by column chromatography on a neutral alumina with a mixture of CH_3CN -toluene (3:1, v/v) as eluant. The mainly red band was collected. The solvent was removed under reduced pressure and a red powder was obtained. Yield: 70%. *Anal. Calc.* for $\text{C}_{39}\text{H}_{29}\text{N}_9\text{Cl}_2\text{O}_9\text{Ru}$: C, 49.85; H, 3.11; N, 13.42. Found: C, 50.28; H, 3.54; N, 13.48%. ESI-MS [CH_3CN , m/z]: 739.7 ($[\text{M}-2\text{ClO}_4-\text{H}]^+$),

370.4 ($[\text{M}-2\text{ClO}_4]^{2+}$). ^1H NMR (500 MHz, $\text{DMSO}-d_6$): δ 8.88 (t, 4H, $\text{H}_{3,3'}$, $J = 5.0$ Hz), 8.84 (d, 2H, H_c , $J = 8.0$ Hz), 8.21 (t, 2H, H_4 , $J = 7.0$ Hz), 8.11 (t, 2H, H_4' , $J = 7.0$ Hz), 7.88 (d, 2H, H_a , $J = 8.0$ Hz), 7.80 (d, 2H, H_6 , $J = 7.8$ Hz), 7.74 (d, 2H, H_6' , $J = 7.7$ Hz), 7.65 (d, 1H, H_f , $J = 7.5$ Hz), 7.59 (t, 4H, $\text{H}_{5,5'}$, $J = 5.0$ Hz), 7.36 (t, 2H, H_b , $J = 6.0$ Hz), 6.63 (d, 1H, H_e , $J = 8.5$ Hz), 6.48 (d, 1H, H_b , $J = 7.5$ Hz), 4.52 (s, 1H, H_{OH}), 3.37 (s, 2H, H_{NH_2}).

Caution: Perchlorate salts of metal compounds with organic ligands are potentially explosive, and only small amounts of the material should be prepared and handled with great care.

2.3. DNA-binding studies

The DNA-binding and photoactivated cleavage experiments were performed at room temperature. Buffer A (5 mM tris-(hydroxymethyl)aminomethane (Tris) hydrochloride, 50 mM NaCl, pH 7.0) was used for absorption titration, luminescence titration and viscosity measurements. Buffer B (50 mM Tris-HCl, 18 mM NaCl, pH 7.2) was used for DNA photocleavage experiments. Buffer C (1.5 mM Na_2HPO_4 , 0.5 mM NaH_2PO_4 , 0.25 mM Na_2EDTA , pH 7.0) was used for thermal DNA denaturation experiments. Buffer D (0.9% of physiological saline) was used for retardation assay of pGL 3 plasmid DNA.

The absorption titrations of the complex in buffer were performed using a fixed concentration (20 μM) for complex to which increments of the DNA stock solution were added. Ru-DNA solutions were allowed to incubate for 5 min before the absorption spectra were recorded. The intrinsic binding constants K , based on the absorption titration, were measured by monitoring the changes of absorption in the MLCT band with increasing concentration of DNA using the following equation [26]:

$$[\text{DNA}]/(\varepsilon_a - \varepsilon_f) = [\text{DNA}]/(\varepsilon_b - \varepsilon_f) + 1/[K_b(\varepsilon_b - \varepsilon_f)] \quad (1)$$

where $[\text{DNA}]$ is the concentration of DNA in base pairs, ε_a , ε_f and ε_b correspond to the apparent absorption coefficient $\text{Aobsd}/[\text{Ru}]$, the extinction coefficient for the free ruthenium complex and the extinction coefficient for the ruthenium complex in the fully bound form, respectively. In plots of $[\text{DNA}]/(\varepsilon_a - \varepsilon_f)$ versus $[\text{DNA}]$, K_b is given by the ratio of slope to the intercept.

Thermal denaturation studies were carried out with a Perkin-Elmer Lambda 35 spectrophotometer equipped with a Peltier temperature-controlling programmer (± 0.1 °C). The melting temperature (T_m) was taken as the mid-point of the hyperchromic transition. The melting curves were obtained by measuring the absorbance at 260 nm for solutions of CT-DNA (80 μM) in the absence and presence of the Ru(II) complex (30 μM) as a function of the temperature. The temperature was scanned from 40 to 90 °C at a speed of 1 °C min^{-1} . The data were presented as $(A - A_0)/(A_f - A_0)$ versus temperature, where A , A_0 , and A_f are the observed, the initial, and the final absorbance at 260 nm, respectively.

Viscosity measurements were carried out using an Ubbelohde viscometer maintained at a constant temperature at 25.0 (± 0.1) °C in a thermostatic bath. DNA samples approximately 200 base pairs in average length were prepared by sonicating in order to minimize complexities arising from DNA flexibility [27]. Flow time was measured with a digital stopwatch, and each sample was measured three times, and an average flow time was calculated. Relative viscosities for DNA in the presence and absence of complexes were calculated from the relation $\eta = (t - t^0)/t^0$, where t is the observed flow time of the DNA-containing solution and t^0 is the flow time of buffer alone [28,29]. Data were presented as $(\eta/\eta)^{1/3}$ versus binding ratio [30], where η is the viscosity of DNA in the presence of complexes and η_0 is the viscosity of DNA alone.

For the gel electrophoresis experiment, supercoiled pBR 322 DNA (0.1 μg) was treated with the Ru(II) complexes in buffer B,

and the solution was then irradiated at room temperature with a UV lamp (365 nm, 10 W). The samples were analyzed by electrophoresis for 1.5 h at 80 V on a 1.0% agarose gel in TBE (89 mM Tris-borate acid, 2 mM EDTA, pH 8.3). The gel was stained with 1 $\mu\text{g}/\text{ml}$ ethidium bromide and photographed on an Alpha Innotech IS-5500 fluorescence chemiluminescence and visible imaging system.

2.4. Cytotoxicity assay

Cytotoxicity of APiP, HAPiP, complexes **1** and **2** was evaluated using standard MTT (3-(4,5-dimethylthiazole)-2,5-diphenyltetrazolium bromide) assay [31]. Cells were placed in 96-well microassay culture plates (8×10^3 cells per well) and grown overnight at 37 °C in a 5% CO_2 incubator. Compounds tested were then added to the wells to achieve final concentrations ranging from 6.25 to 400 μM . Control wells were prepared by addition of culture medium (100 μL). Wells containing culture medium without cells were used as blanks. The plates were incubated at 37 °C in a 5% CO_2 incubator for 48 h. Upon completion of the incubation, stock MTT dye solution (20 μL , 5 mg mL^{-1}) was added to each well. After 4 h incubation, buffer (100 μL) containing *N,N*-dimethylformamide (50%) and sodium dodecyl sulfate (20%) was added to solubilize the MTT formazan. The optical density of each well was then measured on a microplate spectrophotometer at a wavelength of 490 nm. The IC_{50} values were determined by plotting the percentage viability versus concentration on a logarithmic graph and reading off the concentration at which 50% of cells remain viable relative to the control. Each experiment was repeated at least three times to get the mean values. Three different tumor cell lines were the subjects of this study: BEL-7402 (hepatocellular), HepG-2 (hepatocellular) and MCF-7 (breast cancer) (purchased from American Type Culture Collection).

2.5. Apoptosis study

Apoptosis studies were performed with a staining method utilizing acridine orange (AO) and ethidium bromide (EB) [32]. According to the difference in membrane integrity between necrotic and apoptosis. AO can pass through cell membrane, but EB cannot. Under fluorescence microscope, live cells appear green. Necrotic cells stain red but have a nuclear morphology resembling that of viable cells. Apoptosis cells appear green, and morphological changes such as cell blebbing and formation of apoptotic bodies will be observed.

A monolayer of BEL-7402 cells was incubated in the absence or presence of complex **2** at concentration of 50 μM at 37 °C and 5% CO_2 for 48 h. After 48 h, each cell culture was stained with AO/EB solution (100 $\mu\text{g mL}^{-1}$ AO, 100 $\mu\text{g mL}^{-1}$ EB). Samples were observed under a fluorescence microscope.

2.6. Cellular uptake

Cells were placed in 24-well microassay culture plates (4×10^4 cells per well) and grown overnight at 37 °C in a 5% CO_2 incubator. Complexes tested were then added to the wells. The plates were incubated at 37 °C in a 5% CO_2 incubator for 48 h. Upon completion of the incubation, the wells were washed three times with phosphate buffered saline (PBS), after removing the culture media in the wells. The cells were visualized by fluorescent microscopy.

2.7. Scavenger measurements of hydroxyl radical ($\cdot\text{OH}$)

Scavenger measurements of hydroxyl radical ($\cdot\text{OH}$) were carried out in aqueous media. The hydroxyl radical ($\cdot\text{OH}$) was generated by the Fenton system [33]. The solution of the tested complexes was

prepared with DMF (*N,N*-dimethylformamide). The 5 ml of assay mixture contained following reagents: safranin (28.5 μM), EDTA-Fe(II) (100 μM), H_2O_2 (44.0 μM), the tested compounds (0.5–4.5 μM) and a phosphate buffer (67 mM, pH 7.4). The assay mixtures were incubated at 37 $^\circ\text{C}$ for 30 min in a water bath. After which, the absorbance was measured at 520 nm. All the tests were run in triplicate and expressed as the mean. A_i was the absorbance in the presence of the tested compound; A_0 was the absorbance in the absence of tested compounds; A_c was the absorbance in the absence of tested compound, EDTA-Fe(II), H_2O_2 . The suppression ratio (η_a) was calculated on the basis of $(A_i - A_0)/(A_c - A_0) \times 100\%$.

3. Results and discussion

3.1. Viscosity measurements

To investigate the DNA-binding mode of complexes **1** and **2**, viscosity measurements on solutions of CT DNA incubated with the complexes were carried out. It is well known that a classical intercalation of a ligand into DNA is known to cause a significant increase in the viscosity of a DNA solution due to an increase in the separation of the base pairs at the intercalative site and, hence, an increase in the overall DNA molecular length [29]. Fig. 1 shows the change in the relative viscosity of CT DNA on addition of complexes **1** and **2** together with those of $[\text{Ru}(\text{bpy})_3]^{2+}$. It is well known complex $[\text{Ru}(\text{bpy})_3]^{2+}$ to bind with DNA only through electrostatic mode. No obvious effect of $[\text{Ru}(\text{bpy})_3]^{2+}$ on the relative viscosity of the DNA solution was observed. On increasing the amounts of complexes **1** and **2**, the relative viscosity of CT DNA solution increase steadily. These results suggest that complexes **1** and **2** intercalate between the base pairs of DNA. Similar results were also observed for the other complexes [34–36].

3.2. Absorption spectra titration

Electronic absorption spectroscopy is one of the most useful techniques for DNA-binding studies of metal complexes [37,38]. The absorption spectra of the complexes **1** and **2** (20 μM) in the presence of CT DNA are shown in Fig. 2. As the DNA concentration is increased, the MCLT (metal-to-ligand charge transfer) transition bands of complexes **1** at 458 and **2** at 459 nm exhibit hypochromism of about 30.48 and 17.87%, and bathchromism of 2 and 3 nm, respectively. These spectral characteristics may suggest a mode of binding that involves a stacking interaction between the aromatic chromophore and the DNA base pairs. In order to elucidate the binding strength of the complexes, the DNA-binding constants K were determined by monitoring the changes of

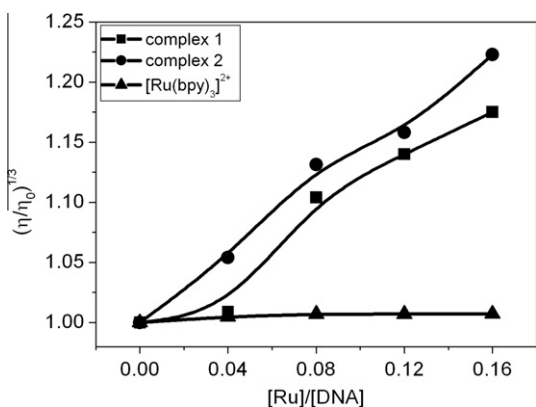


Fig. 1. Effect of increasing amounts of complexes $[\text{Ru}(\text{bpy})_3]^{2+}$ (\blacktriangle), **1** (\blacksquare) and **2** (\bullet) on the relative viscosity of calf thymus DNA at 25 (± 0.1) $^\circ\text{C}$. $[\text{DNA}] = 0.25$ mM.

absorbance in the MLCT band with increasing concentration of CT DNA. The values of K are $6.08 (\pm 0.29) \times 10^4 \text{ M}^{-1}$ and $1.78 (\pm 0.29) \times 10^5 \text{ M}^{-1}$ for **1** and **2**. It is obvious that the K values of complexes **1** and **2** are comparable with those of other known DNA-intercalative complexes: $[\text{Ru}(\text{NH}_3)_4(\text{dppz})]^{2+}$ (1.24×10^5) [39], $[\text{Ru}(\text{bpy})_2(\text{PPiP})]^{2+}$ ($4.30 \times 10^4 \text{ M}^{-1}$) [40] and $[\text{Ru}(\text{dmb})_2(\text{DBHIP})]^{2+}$ ($8.64 \pm 0.16 \times 10^4 \text{ M}^{-1}$) [41], but is not as large as that of classical DNA-intercalator $[\text{Ru}(\text{bpy})_2(\text{dppz})]^{2+}$ ($4.90 \times 10^6 \text{ M}^{-1}$) [42].

3.3. Luminescence spectra

The luminescence spectra have been confirmed to be effective for characterizing the binding mode of the metal complexes to DNA [43,44]. Complexes **1** and **2** can emit luminescence in Tris-HCl buffer at ambient temperature with a maximum appearing at 599 and 600 nm. The enhancements in the emission intensity of complexes **1** and **2** with increasing CT DNA concentrations are given in Fig. 3. Upon addition of DNA, the emission intensities of complexes **1** and **2** increase about 1.63 and 1.88 times larger than the original and saturate at a ration of $[\text{DNA}]/[\text{Ru}] = 15.4$ and 14.6, respectively. The phenomenon was related to the extent to which the complexes penetrate into the hydrophobic environment inside the DNA, thereby avoiding the quenching effect of solvent water molecules. The binding constants of the complexes interacting with DNA from the emission spectra can be derived using the luminescence titration method. The binding data obtained from the emission spectra were fitted using the McGhee and von Hippel equation [45] to acquire the binding parameters. The intrinsic binding constants K_b of $2.91 (\pm 0.22) \times 10^4$ ($s = 1.01$) and $3.19 (\pm 0.18) \times 10^5 \text{ M}^{-1}$ ($s = 1.05$) for complexes **1** and **2** were determined. Comparing with that obtained from absorption spectra, the binding constants obtained from luminescence titration with McGhee–von Hippel method are the same magnitude with that obtained from absorption titration method.

3.4. Thermal denaturation study

Generally, the melting temperature of DNA increases when metal complexes bind to DNA by intercalation, as intercalation of complexes between DNA base pairs can cause stabilization of base stacking and hence raises the melting temperature of double-strand DNA. As is shown in Fig. 4, in the absence of any added complexes, the thermal denaturation carried out for DNA gave a T_m of 61.59 ± 0.5 $^\circ\text{C}$ under our experimental conditions. In the presence of complexes **1** and **2**, the T_m is 66.66 ± 0.5 and 68.23 ± 0.5 $^\circ\text{C}$. The melting point increased by +5.07 for complex **1** and +6.64 $^\circ\text{C}$ for complex **2**. The increase in T_m of DNA with the two Ru(II) complexes are comparable to those observed for classical intercalators [46,47].

3.5. Photocleavage by Ru(II) complexes

It is well known that DNA cleavage is controlled by relaxation of supercoiled circular conformation of pBR 322 DNA to nicked circular and/or linear conformations. When electrophoresis is applied to circular plasmid DNA, the fastest migration will be observed for DNA of closed circular conformation (Form I). If one strand is cleaved, the supercoil will relax to product a slower moving nicked conformation (Form II). If both strands are cleaved, a linear conformation (Form III) will be generated that migrates in between. As shown in Fig. 5, no obvious cleavage was observed for the control in which metal complexes was absent (DNA alone), or incubation of the plasmid with the Ru(II) complexes in the dark. With increasing concentration of complexes, the Form I decrease and Form II

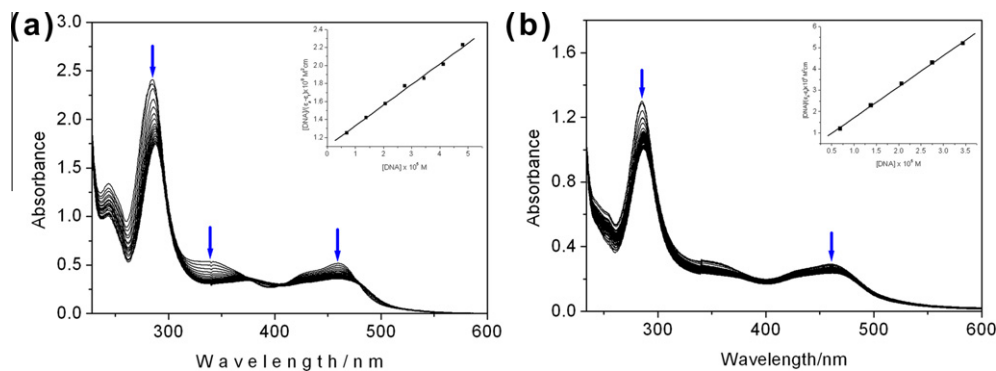


Fig. 2. Absorption spectra of complex **1** (a) and **2** (b) in Tris–HCl buffer upon addition of CT-DNA. [Ru] = 20 μ M. Arrow shows the absorbance change upon the increase of DNA concentration. Plots of $[DNA]/(\epsilon_a - \epsilon_f)$ versus $[DNA]$ for the titration of DNA with Ru(II) complexes.

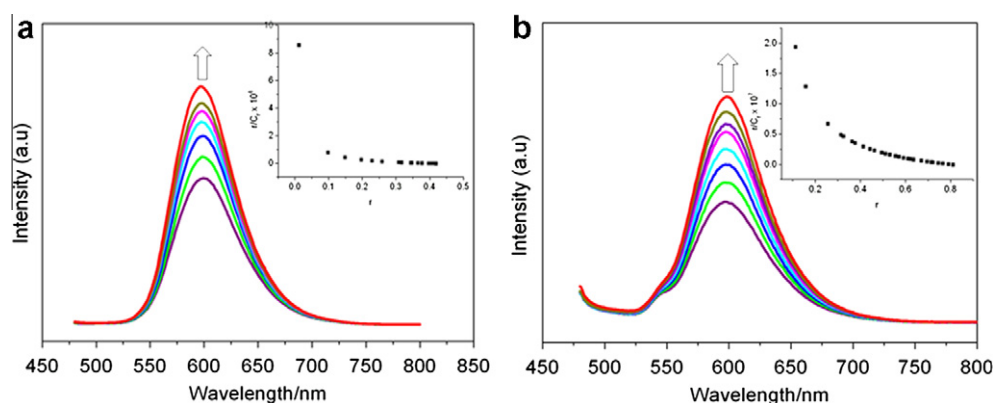


Fig. 3. Luminescence spectra of complexes **1** (a) and **2** (b) in Tris–HCl buffer upon addition of CT DNA. [Ru] = 5 μ M. Arrow shows the intensity change upon the increase of DNA concentration. Inset: Scatchard plot of each complex.

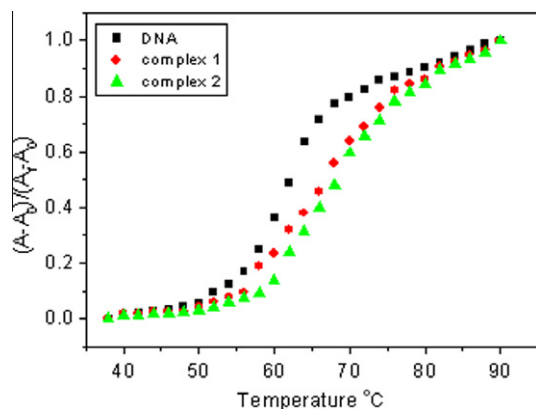


Fig. 4. Thermal denaturation of CT DNA in the absence (■) and presence of complexes **1** (●) and **2** (▲). [Ru] = 30 μ M, [DNA] = 80 μ M.

increase gradually. At the concentration of 16 μ M, both complexes can completely cleave the plasmid DNA.

To investigate the role of radicals in the DNA cleavage by the complexes, reactions were carried out by incubating the complexes **1** and **2** with DNA in presence of hydroxyl radical scavengers (*D*-mannitol and DMSO), singlet oxygen scavenger (*L*-histidine), and a superoxide scavenger (superoxide dismutase, SOD). Fig. 6 shows that the DNA cleavage of the plasmid by complexes **1** and **2** was not inhibited in the presence of hydroxyl radical (\cdot OH) scavengers such as mannitol and DMSO, which indicated that hydroxyl radical was not likely to be the cleaving agent. In the presence of SOD, a facile superoxide anion radical ($O_2^{\cdot-}$) quencher, the cleavage

of DNA was improved. Partial inhibition of DNA cleavage was observed in presence of histidine, suggesting that 1O_2 is likely to be the reactive species responsible for the cleavage reaction. These results demonstrate that superoxide anion radical ($O_2^{\cdot-}$) and singlet oxygen (1O_2) may play important role in the cleavage of the plasmid DNA.

3.6. Condensation of pGL 3 plasmid DNA by Ru(II) complexes

When the positively charged cationic metal complexes meet the negatively charged plasmid DNA, adduct of complex-DNA is formed by the condensation process between the metal complexes and DNA. The abilities of cationic metal complexes to condense plasmid DNA into particular structure is a primary prerequisite for efficient gene transfection and cellular uptake. In order to evaluate the abilities of complexes **1** and **2** to condense DNA, the retardation of pGL 3 plasmid DNA was performed. Fig. 7 shows when the concentrations of complexes **1** and **2** are 1 and 2 mM, both complexes cannot condense the DNA, however, at high concentrations of 6 mM for complex **1**, or 4 and 6 mM for complex **2**, the effects of condensation of DNA were obviously observed.

3.7. Cytotoxicity assay in vitro

The potential antiproliferative effects of complexes **1** and **2** on the viability of tumor cell lines (BEL-7402, HepG-2, and MCF-7) were detected by the MTT assay. Cisplatin was used as a positive control. The concentrations which showed 50% (IC_{50}) inhibition of the cell viability were calculated and the results were listed in

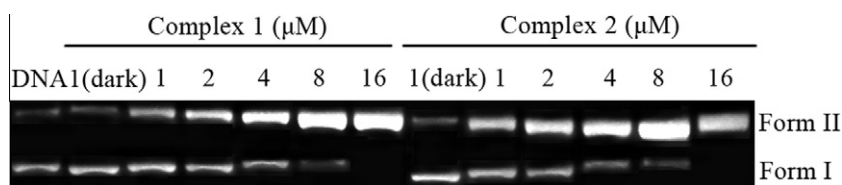


Fig. 5. Photoactivated cleavage of pBR 322 DNA in the presence of different concentrations of Ru(II) complexes after irradiation at 365 nm for 30 min.

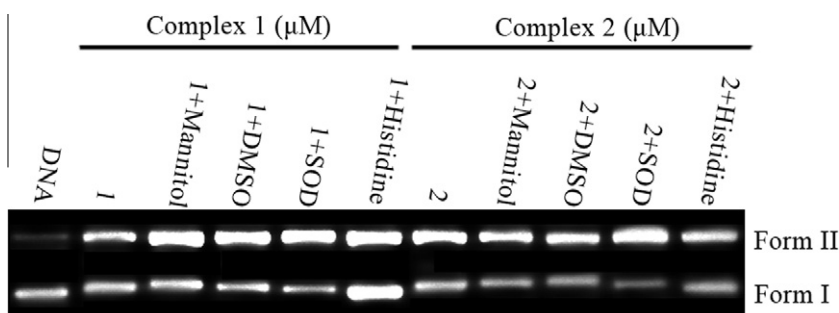


Fig. 6. Photoactivated cleavage of supercoiled pBR 322 DNA by complexes **1** and **2** (20 μM) in the absence and presence of different inhibitors [100 mM mannitol, 200 mM dimethyl sulfoxide (DMSO), 1000 U ml^{-1} superoxide dismutase (SOD), 1.2 mM distidine] after irradiation at 365 nm for 30 min.

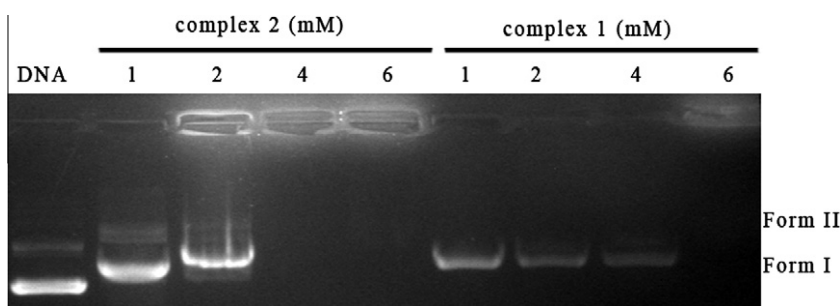


Fig. 7. Agarose gel electrophoresis retardation of pGL3 plasmid DNA in the presence different concentrations of complex **1** and **2**. [DNA] = 0.5 μg .

Table 1
The IC_{50} values for complexes **1**, **2** and cisplatin against selected cell lines.

Complex	IC_{50} (mM)		
	BEL-7402	HepG-2	MCF-7
1	0.492	0.313	0.215
2	0.197	0.097	0.118
Cisplatin	0.019	0.025	0.012

Table 1. The IC_{50} values for complex **2** (0.197, 0.097 and 0.118 mM on BEL-7402, HepG-2 and MCF-7, respectively) are far lower than that of complex **1** (0.492, 0.313 and 0.215 mM) under the identical condition. It is clear that complex **2** is more sensitive against the selected tumor cell lines than complex **1**, but these complexes all exhibit relatively lower in vitro cytotoxicity against the selected cell lines than cisplatin. The results showed that the cytotoxicity of complexes **1** and **2** was found to be concentration dependent, and the cell viability decreased with increasing the concentrations of ruthenium(II) complexes.

3.8. Apoptotic activity

Apoptosis plays a major role during the development and homeostasis. Apoptosis is a form of programmed cell death which occurs through the activation of the cell-intrinsic suicide machinery. And apoptosis is primarily a physiological process necessary

to remove individual cells that are no longer needed or that function abnormally [48]. Apoptosis assays were performed with a staining method utilizing acridine orange (AO) and ethidium bromide (EB). The AO/EB staining is sensitive to DNA and was used to assess changes in nuclear morphology. Apoptotic cells will show apoptotic features such as nuclear shrinkage, chromatin condensation. In the absence of complex **2** (50 μM), the living cells were stained bright green in spots (Fig. 8A). However, apoptotic and necrotic cells can be distinguished from one another using fluorescence microscope after being stained with AO/EB solution. After treatment of BEL-7402 cell line with complex **2**, green apoptotic cells containing apoptotic bodies, as well as red necrotic cells, were observed (Fig. 8B). Similar result for complex **1** was also observed. The percentage (%) of necrotic and apoptotic cell of BEL-7402 cells in the presence of different concentration of complexes **1** and **2**. The results were depicted in Fig. 9. As increasing concentrations of complexes **1** and **2**, the ratios of apoptotic versus necrotic cells are 0.13, and 0.14 for **1**, 1.59 and 4.07 for **2**. The results showed the number of apoptotic cells increased obviously with increasing concentration of complex **2**.

3.9. Cellular uptake studies

The uptake of the complexes **1** and **2** by cells was studied with Human hepatocellular carcinoma cell line (BEL-7402). Complex **2** (50 μM) was added to the wells (4×10^4 cells per well). The plates

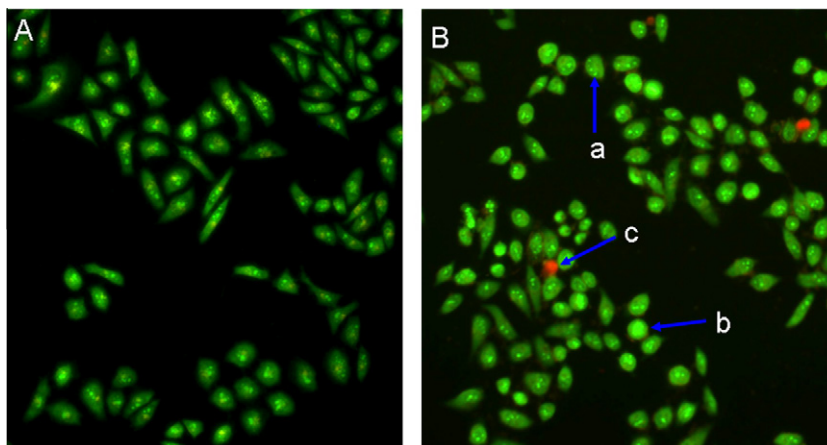


Fig. 8. BEL-7402 cells were stained by AO/EB and observed under fluorescence microscopy. BEL-7402 cells without treatment (A) and in the presence of complex 2 (B) incubated at 37 °C and 5% CO₂ for 48 h. cells in a, b and c are living, apoptotic and necrotic cells, respectively.

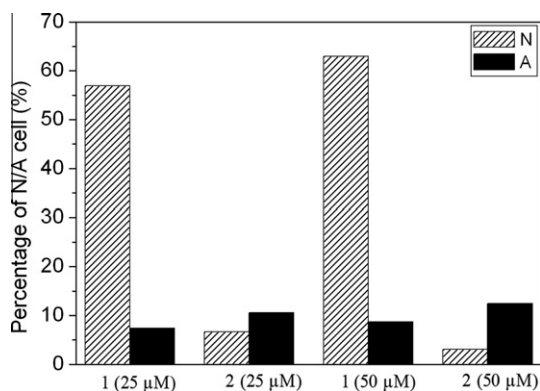


Fig. 9. The percentage (%) of necrotic (N) and apoptotic (A) cell of BEL-7402 cells incubated with different concentrations of complexes 1 and 2 for 24 h by flow cytometry.

were incubated at 37 °C in a 5% CO₂ incubator for 48 h. Upon completion of the incubation, the wells were washed three times with phosphate buffered saline (PBS), after removing the culture media, the cells were observed under fluorescent microscope. As shown in Fig. 10A and B, the bright red fluorescent spots in the images were observed. The results show that complexes 2 can be uptaken by cells, and they can enter into the cytoplasm and accumulate in the nuclei. Similar result for complex 1 (25 μM) was also observed.

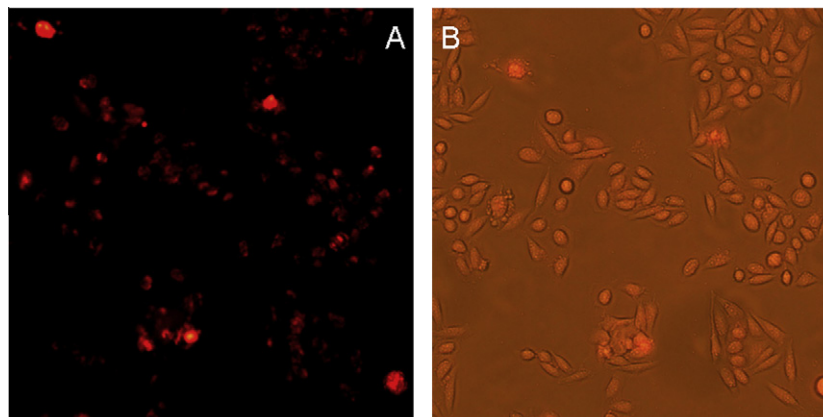


Fig. 10. BEL-7402 cells incubated with complex 2 (50 μM) for 48 h imaged by fluorescence microscopy. (A) Imaged under fluorescence, (B) imaged under fluorescence and visible light. Note that the cytoplasm is extensively stained with the Ru(II) complexes.

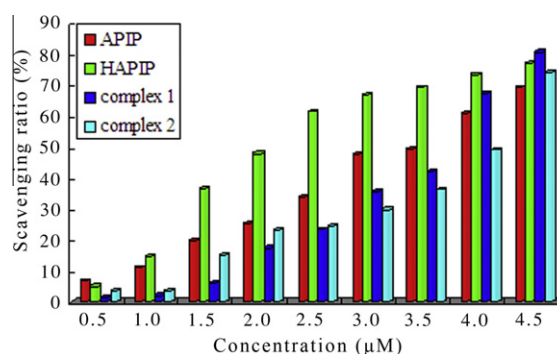


Fig. 11. Scavenging effect of the ligands and complexes on hydroxyl radicals. Experiments were performed in triplicate.

3.10. Antioxidant activity against hydroxyl radical ($\cdot\text{OH}$)

Various oxygen species occur during the metabolizable process of biological systems. Superoxide anion radical ($\text{O}_2^{\cdot-}$) and hydroxyl radical ($\cdot\text{OH}$) are presumed to play an important role in a number of biological phenomena such as aging, coronary heart disease, rheumatoid arthritis, cancer and other pathological conditions. The hydroxyl radical ($\cdot\text{OH}$) is by far the most potent and therefore the most dangerous oxygen metabolite, elimination of this radical is one of the major aims of antioxidant administration [49]. The

Table 2
Scavenging ratio (%) of ligands and complexes against ·OH.

Comp	Average inhibition (%) for ·OH								
	0.5 (μM)	1.0 (μM)	1.5 (μM)	2.0 (μM)	2.5 (μM)	3.0 (μM)	3.5 (μM)	4.0 (μM)	4.5 (μM)
APIP	6.59	10.85	19.76	25.19	33.72	47.28	52.92	60.46	68.99
HAPIP	4.96	14.54	36.52	47.52	61.35	66.67	68.76	73.05	76.60
1	1.13	1.88	6.04	17.36	23.39	35.47	41.88	67.17	80.38
2	3.56	3.59	14.70	22.88	24.50	29.74	36.27	48.74	73.85

hydroxyl radical (·OH) in aqueous media was generated by the Fenton system. The antioxidant activity of ligands, APIP and HAPIP and their complexes **1** and **2** were investigated. Fig. 11 depicts the inhibitory effect of ligands and complexes on ·OH. The average suppression ratio against ·OH (Table 2) valued from 6.59% to 72.86% for APIP, 4.96% to 82.27% for HAPIP, 1.13% to 93.96% for complex **1**, and 3.59% to 77.45% for complex **2**. The antioxidant activity against hydroxyl radical of complex **1** appeared higher than that of complex **2** at the concentration range (from 3.0 to 4.5 μM) under the same experimental condition. For complex **1**, the hydroxyl radical scavenging ability can be enhanced when ligand (APIP) bonds metal center to form complex at high concentrations. However, the antioxidant activity of ligand (HAPIP) is weakened when it bonds metal center to form complex **2**. These results suggest that ligands and their complexes may be potential drugs to eliminate the hydroxyl radical.

4. Conclusion

Two new ligands APIP, HAPIP and relative two ruthenium(II) complexes [Ru(bpy)₂(APIP)]²⁺ and [Ru(bpy)₂(HAPIP)]²⁺ were synthesized and characterized. The DNA-binding behaviors show these complexes interact with CT DNA by intercalation. Complexes **1** and **2** can inhibit the proliferation of the selected cell lines in different degree. Apoptotic assay suggests that complexes **1** and **2** can induce apoptosis. The cellular uptake shows these complexes can enter into the cytoplasm and accumulate in the nuclei. Upon irradiation at 365 nm, complexes **1** and **2** can cleave the plasmid DNA. The studies on the mechanism of photocleavage demonstrate that superoxide anion radical (O₂^{·-}) and singlet oxygen (¹O₂) may play an important role. At high concentration, complexes **1** and **2** can effectively condense the pGL 3 DNA. The antioxidant experiments against hydroxyl radical show the ligands and complexes possess excellent antioxidant abilities.

Acknowledgements

This work was supported by the National Nature Science Foundation of China (Nos. 31070858 and 30800227) and Guangdong Pharmaceutical University for financial supports.

References

- [1] U. Schatzschneider, J. Niesel, I. Ott, R. Gust, H. Alborzina, S. Wöfl, ChemMedChem 3 (2008) 1104.
- [2] L.F. Tan, J.L. Shen, X.J. Chen, X.L. Liang, DNA Cell Biol. 28 (2009) 461.

- [3] Y.J. Liu, C.H. Zeng, Z.H. Liang, J.H. Yao, H.L. Huang, Z.Z. Li, F.H. Wu, Eur. J. Med. Chem. 45 (2010) 3087.
- [4] S. Shi, X.T. Geng, J. Zhao, T.M. Yao, C.R. Wang, D.J. Yang, L.F. Zheng, L.N. Ji, Biochimie 92 (2010) 370.
- [5] J. Tan, B.C. Wang, L.C. Zhu, Bioorg. Med. Chem. 17 (2009) 614.
- [6] M. Roy, R. Santhanagopal, A.R. Chakravarty, Dalton Trans. (2009) 1024.
- [7] Q. Wang, Z.Y. Yang, G.F. Qi, D.D. Qin, Biometals 22 (2009) 927.
- [8] G. Zuber, J.C. Quada, S.M. Hecht Jr., J. Am. Soc. Chem. 120 (1998) 9368.
- [9] S.M. Hecht, J. Nat. Prod. 63 (2000) 158.
- [10] A. Sigel, H. Sigel (Eds.), vol. 33, Marcel Dekker, New York, 1996, p. 177.
- [11] L.N. Ji, X.H. Zou, J.G. Liu, Coord. Chem. Rev. 216–217 (2001) 513.
- [12] V.G. Vaidyanathan, B.H. Nair, Dalton Trans. (2005) 2842.
- [13] P.P. Pelligrini, J.P. Aldrich-Wright, Dalton Trans. (2003) 176.
- [14] P.U. Maheswari, M. Palaniandavar, Inorg. Chim. Acta 357 (2004) 901.
- [15] P. Lincoln, B. Norden, Int. Pat., WO 99/15535, 1999.
- [16] J. Liu, X.H. Zou, Q.L. Zhang, W.J. Mei, J.Z. Liu, L.N. Ji, Met.-Based Drugs 7 (2000) 343.
- [17] C.A. Puckett, J.K. Barton, J. Am. Chem. Soc. 129 (2007) 46.
- [18] D.L. Ma, C.M. Che, F.M. Siu, M. Yang, K.Y. Wong, Inorg. Chem. 46 (2007) 740.
- [19] G.L. Pascu, A.C.G. Hotze, C. Sanchez-Cano, B.M. Kariuki, M.J. Hannon, Angew. Chem. 119 (2007) 4452.
- [20] T.R. Krugh, J.W. Neely, Biochemistry 12 (1973) 4418.
- [21] J. Marmur, J. Mol. Biol. 3 (1961) 208.
- [22] M.E. Reichmann, S.A. Rice, C.A. Thomas, P. Doty, J. Am. Chem. Soc. 76 (1954) 3047.
- [23] Y. Xiong, X.F. He, X.H. Zou, J.Z. Wu, X.M. Chen, L.N. Ji, R.H. Li, J.Y. Zhou, K.B. Yu, J. Chem. Soc., Dalton Trans. 1 (1999) 19.
- [24] J.G. Liu, B.H. Ye, H. Chao, Q.X. Zhen, L.N. Ji, Chem. Lett. 28 (1999) 1085.
- [25] B.P. Sullivan, D.J. Salmon, T.J. Meyer, Inorg. Chem. 17 (1978) 3334.
- [26] A. Wolf, G.H. Shimer Jr., T. Meehan, Biochemistry 26 (1987) 6392.
- [27] J.B. Chaires, N. Dattagupta, D.M. Crothers, Biochemistry 21 (1982) 3933.
- [28] A.E. Friedman, J.C. Chambron, J.P. Sauvage, N.J. Turro, J.K. Barton, J. Am. Chem. Soc. 112 (1990) 4960.
- [29] S. Satyanarayana, J.C. Dabrowiak, J.B. Chaires, Biochemistry 31 (1993) 9319.
- [30] G. Cohen, H. Eisenberg, Biopolymers 8 (1969) 45.
- [31] T.J. Mosmann, Immunol. Methods 65 (1983) 55.
- [32] D.L. Specter, R.D. Goldman, L.A. Leinwand, In cells: a laboratory manual, vol. 1, Cold Spring Harbor Laboratory Press, New York, 1998 (Chapter 15).
- [33] C.C. Winterbourn, Free Radic. Biol. Med. 3 (1987) 33.
- [34] S. Satyanarayana, J.C. Dabrowiak, J.B. Chaires, Biochemistry 32 (1993) 2573.
- [35] H.L. Huang, Y.J. Liu, C.H. Zeng, L.X. He, F.H. Wu, DNA Cell Biol. 29 (2010) 261.
- [36] Q. Wang, Q. Z.Y. Yang, G.F. Qi, D.D. Qin, Eur. J. Med. Chem. 44 (2009) 2425.
- [37] Y.J. Liu, C.H. Zeng, J.H. Yao, F.H. Wu, L.X. He, H.L. Huang, Chem. Biodivers. 7 (2010) 1770.
- [38] J.K. Barton, A. Danishefsky, J. Goldberg, J. Am. Chem. Soc. 106 (1984) 2172.
- [39] X.Q. He, Q.Y. Lin, R.D. Hu, Spectrochim. Acta, Part A 68 (2007) 184.
- [40] R.B. Nair, E.S. Teng, S.L. Kirkland, C.J. Murphy, Inorg. Chem. 37 (1998) 139.
- [41] L.F. Tan, H. Chao, Y.J. Liu, B. Sun, W. Wei, L.N. Ji, J. Inorg. Biochem. 99 (2005) 513.
- [42] Y.J. Liu, Z.H. Liang, Z.Z. Li, C.H. Zeng, J.H. Yao, H.L. Huang, F.H. Wu, Biometals 23 (2010) 739.
- [43] C. Zhao, H. Lin, S. Zhu, H. Sun, Y. Chen, J. Inorg. Biochem. 70 (1998) 219.
- [44] M. Howe-Grant, K.C. Wu, W.R. Bauer, S.J. Lippart, Biochemistry 15 (1976) 4339.
- [45] J.D. McGhee, P.H. von Hippel, J. Mol. Biol. 86 (1974) 469.
- [46] M.J. Waring, J. Mol. Biol. 13 (1965) 269.
- [47] G.A. Neyhart, N. Grover, S.R. Smith, W.A. Kalsbeck, T.A. Fairly, M. Cory, H.H. Thorp, J. Am. Chem. Soc. 115 (1993) 4423.
- [48] D. Vinatier, P.H. Dufour, D. Subtil, Eur. J. Obstet. Gyn. RB 67 (1996) 85.
- [49] U. Udilova, A.V. Kozlov, W. Bieberschulte, K. Frei, K. Ehrenberger, H. Nohl, Biochem. Pharm. 65 (2003) 59.